Journal of Sports Sciences
Publication details, including instructions for authors and subscription information:
http://www.tandfonline.com/loi/rjsp20

From block clearance to sprint running: Characteristics underlying an effective transition

Sofie Debaere [a], Christoph Delecluse [a], Dirk Aerenhouts [b], Friso Hagman [b] & Ilse Jonkers [a]
[a] Department of Kinesiology, Faculty of Kinesiology and Rehabilitation Sciences, Katholieke Universiteit Leuven, Leuven, Belgium
[b] Department of Human Biometry and Biomechanics, Vrije Universiteit Brussel, Brussels, Belgium
Published online: 13 Sep 2012.

To cite this article: Sofie Debaere, Christoph Delecluse, Dirk Aerenhouts, Friso Hagman & Ilse Jonkers (2013) From block clearance to sprint running: Characteristics underlying an effective transition, Journal of Sports Sciences, 31:2, 137-149, DOI: 10.1080/02640414.2012.722225

To link to this article: http://dx.doi.org/10.1080/02640414.2012.722225

Journal of Sports Sciences, 2013
Vol. 31, No. 2, 137–149, http://dx.doi.org/10.1080/02640414.2012.722225

Routledge
Taylor & Francis Group

From block clearance to sprint running: Characteristics underlying an effective transition

SOFIE DEBAERE[1], CHRISTOPH DELECLUSE[1], DIRK AERENHOUTS[2], FRISO HAGMAN[2], & ILSE JONKERS[1]

[1]*Department of Kinesiology, Faculty of Kinesiology and Rehabilitation Sciences, Katholieke Universiteit Leuven, Leuven, Belgium and* [2]*Department of Human Biometry and Biomechanics, Vrije Universiteit Brussel, Brussels, Belgium*

(Accepted 15 August 2012)

Abstract
The aim of this study was to characterize the specifics of the sprint technique during the transition from start block into sprint running in well-trained sprinters. Twenty-one sprinters (11 men and 10 women), equipped with 74 spherical reflective markers, executed an explosive start action. An opto-electronic motion analysis system consisting of 12 MX3 cameras (250 Hz; 325,000 pixels) and two Kistler force plates (1000 Hz) was used to collect the three-dimensional (3D) marker trajectories and ground reaction forces (Nexus, Vicon). The 3D kinematics, joint kinetics, and power were calculated (Opensim) and were time normalized to 100% from the first action after gunshot until the end of second stance after block clearance (Matlab). The results showed that during the first stance, power generation at the knee plays a significant role in obtaining an effective transition, representing 31% of power generation in the lower limb, in the absence of preceding power absorption. Furthermore, the sprinter actively searches a more forward leaning position to maximize horizontal velocity. Since success during sprinting from the second stance onwards involves high hip and ankle activation, the above-mentioned three characteristics are specific skills required to successfully conclude the transition from start block into sprint running.

Keywords: *Sprint start, biomechanics, 3D motion analysis, well-trained athletes*

Introduction

Optimal performance in sprinting depends on attaining maximal horizontal power during block clearance and on increasing velocity from block clearance into sprint running (Bezodis, Salo, & Trewartha, 2010; Golden, Pavol, & Hoffman, 2009). During this transition phase, the athlete aims to maximize forward velocity while controlling upward and medio-lateral velocity. This depends on specific technical skills that enable development of forward velocity from set position in the blocks into an extended position on block clearance. Meanwhile, the centre of mass rises gradually and the trunk partially maintains its forward leaning position.

For the different phases of the sprint, technical skills to successfully conclude the block action and initiate running action are already documented in terms of muscle coordination and consequent interaction between the different segments (Charalambous, Irwin, Bezodis, & Kerwin, 2012; Coh & Tomazin, 2006; Jacobs, 1992; Mero, 2006; Slawinski et al., 2010a, 2010b). Peak power generation at hip, knee, and ankle joint occurs in a proximal-to-distal time sequence during both first and second stance after block clearance (Charalambous et al., 2012; Jacobs, 1992) and during sprinting at maximal velocity (Bezodis, Kerwin, & Salo, 2008; Mann & Sprague, 1980; Mann, 1981). The contribution of the knee to power generation differs between phases: a knee extensor action is seen during take-off of the first stance, whereas only small knee moment and power values are observed during sprinting at maximal velocity. In contrast, major periods of power generation of the hip extensors in early stance and of the ankle plantar flexors are observed (Bezodis et al., 2008; Charalambous et al., 2012). Jacobs and colleagues concluded that the sprinter moves the body centre of mass forward by pivoting around the forefoot before extending the lower limb (Jacobs, 1992; Jacobs, Bobbert, & Van Inghen Schenau, 1996). There is, however, a lack of knowledge

Correspondence: I. Jonkers, Department of Kinesiology, Faculty of Kinesiology and Rehabilitation Sciences, Katholieke Universiteit Leuven, Tervuursevest 101, B-3001 Leuven, Belgium. E-mail: ilse.jonkers@faber.kuleuven.be

concerning the specific characteristics of the transition from the block action into the running action, including the flight and stance of first and second step after block clearance.

It is known that during the transition phase contact times are larger and flight times shorter compared with steps at maximal velocity (Coh, Milanovic, & Kampmiller, 2001; Hoyt, Wickler, & Cogger, 2000; Salo, Bezodis, Batterham, & Kerwin, 2011). This may reflect the temporal consequences of strategies adopted by the athlete to accelerate from the blocks using dedicated joint kinematics and kinetics representative of phase-specific muscle action. Specific inter-segmental interactions during these initial steps and especially the role of trunk rise and lateral foot positioning in developing initial sprinting velocity require clarification, as both seem to conflict with an optimal control of medio-lateral and upward velocity. As only the time history of forward velocity has been documented previously (Coh, 2006; Coh, Peharec, & Bacic, 2007; Slawinski et al., 2010a), it is essential to describe the development of the upward and medio-lateral velocity.

In addition, biomechanical research on documenting joint kinematics and especially kinetics and exploring their relation with sprinting velocity during this transition phase is essential. Therefore, we will characterize the specific technical skills of well-trained sprinters during the transition from start block into sprint running by providing insights into full three-dimensional kinematic and kinetic characteristics underlying initial sprinting performance during the first steps after block clearance.

Methods

Participants

Twenty-one well-trained sprinters (11 men and 10 women) gave their written consent to participate in the study. Their age, body mass, height, and personal best times over 100 m are presented in Table I. Personal best times over 100 m ranged between 10.51 s and 11.00 s for men and between 11.41 s and 12.07 s for women. Well-trained sprinters were chosen because they are likely to have developed the most effective coordination to handle this transition. The study conformed to the recommendations of the Declaration of Helsinki, and had been approved by the local ethics committee.

Procedures

Testing took place at the beginning of the summer season in a gymnastic hall with a tartan track surface. After an individualized warm-up, all sprinters completed three maximal-effort 10-m sprints, with complete recovery between sprints. The participants wore their own spiked shoes and adjusted the start blocks in the same manner as during competition. Starting commands were identical to those used in competition.

Data collection

Anthropometric data. Following ISAK guidelines (Marfell-Jones, Olds, Steward, & Carter, 2006), standing height was measured to the nearest 0.1 cm using a custom-made, wall-mounted stadiometer, while body mass was measured with a TANITA-TBF 410 weight scale, accurate to 100 g.

Optoelectronic motion capture system. Kinematics was measured using three-dimensional (3D) motion analysis (Vicon, Oxford Metrics, UK). We used 12 MX3 cameras (250 Hz, 325,000 pixels) positioned so as to collect data in the starting block and the first two steps (5 m length) (Figure 1). A full body marker placement protocol was used, consisting of 74 spherical reflective markers (Figure 2), containing eight technical clusters. After a static trial in the T-position (Figure 2), eight medial markers were removed so as not to hinder sprinting.

Force platforms. Ground reaction forces were measured during the first two contacts using two Kistler force plates (1000 Hz) embedded in the track, with the first spanning the whole width of the track and the second only spanning the right side of the track. Therefore, data for the second flight and stance phase are limited to athletes starting with the right foot in front (6 of 21 athletes).

Both systems were recorded synchronously in the Vicon data acquisition system.

Data processing

After initial marker labelling in Nexus (Vicon, Oxford Metrics, UK), a generic musculoskeletal model with 14 segments [head, trunk (HT), pelvis and bilateral upper arm, lower arm, hand, femur, tibia and foot], 26 degrees of freedom, and 92

Table I. Characteristics of the sprinters (mean ± *s*).

	Age (years)	Body mass (kg)	Height (m)	Personal best 100 m (s)
Elite male sprinters	24.3 ± 1.8	77.4 ± 6.0	1.820 ± 0.060	10.62 ± 0.18
Elite female sprinters	22.8 ± 3.9	58.2 ± 6.5	1.711 ± 0.045	11.89 ± 0.30

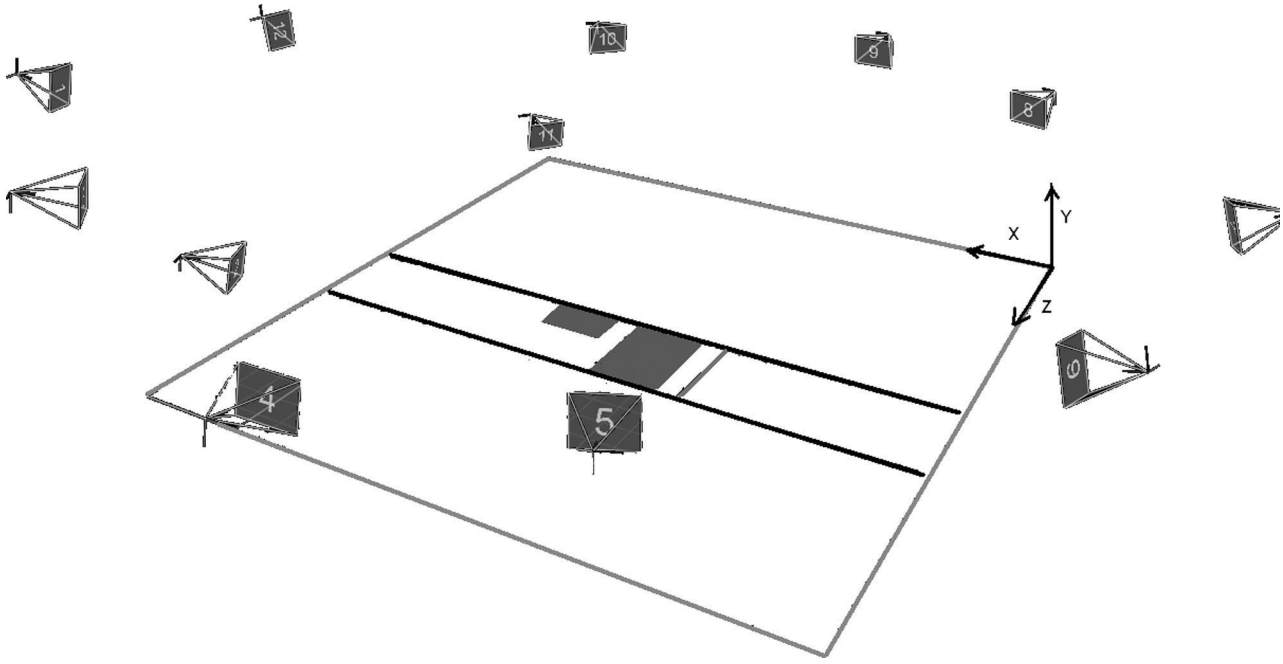

Figure 1. Motion capture set-up.

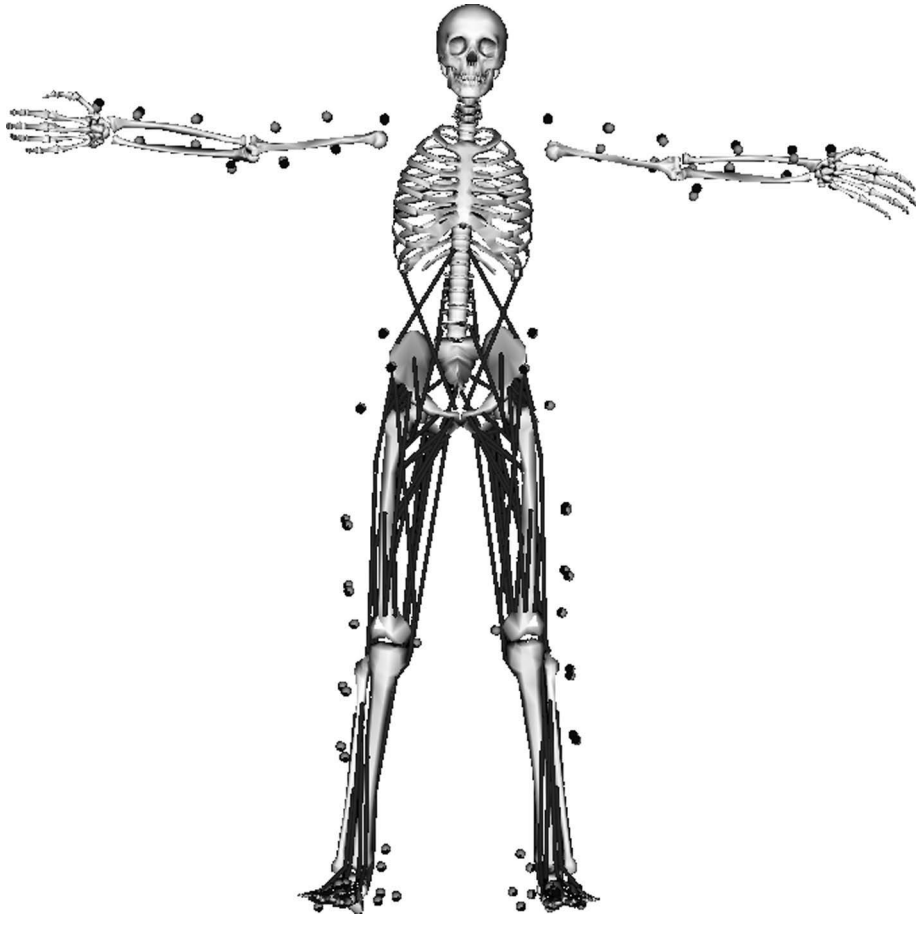

Figure 2. Static trial with body labelled with 74 passive reflective markers: on the processus spinosus of C7; lateral aspect of the acromion bilaterally; lateral and medial elbow; lateral and medial wrist; processus spinosus of L3; spina iliaca anterior superior; spina iliaca anterior inferior; greater trochanter; lateral and medial knee; lateral and medial ankle; heel (2); lateral, medial and middle forefoot; and toe. There are eight technical clusters: mid-humeri, mid-radius, mid-femur, and mid-shank.

muscle-tendon actuators (Hamner, Seth, & Delp, 2010) was scaled to accommodate individual anthropometry based on marker positions obtained during a static trial (Delp et al., 2007). For the head-trunk, the lumbar spine presented three degrees of freedom with respect to the pelvis segment describing flexion/extension, bending, and rotation; the shoulder presented three degrees of freedom of the upper arm with respect to the head-trunk (flexion/extension, abduction/adduction, and exo/endorotation); the elbow presented two degrees of freedom between upper and lower arm (flexion/extension and pronation/supination); the hip was modelled to represent three degrees of freedom (flexion/extension, abduction/adduction, and exo/endorotation); the knee was modelled as one degree of freedom between thigh and shank representing flexion/extension; the ankle was modelled as one degree of freedom representing plantar/dorsiflexion; and movement of the pelvis with respect to the ground was represented by three rotational (tilt, list, and rotation) and three translational degrees of freedom (Hamner et al., 2010).

Based on the 3D marker trajectories during the running trial, an inverse kinematics procedure was conducted to calculate the relevant joint angles. An angle of 180° represented the anatomical position for the hip and knee in flexion/extension. Neutral ankle plantar/dorsiflexion was represented by an angle of 90°. Absolute angles of the pelvis were set to zero if the segment angle coincided with the global X, Y or Z axis of the laboratory coordinate system. For all other angles – hip abduction and rotation, and lumbar extension – the anatomical position is indicated by an angle of zero degrees (Figure 3). Joint angles were low-pass filtered (12 Hz) using a fourth-order Butterworth filter implemented in Matlab (version R2008a, The Mathworks) to adequately suppress motion artefacts without inducing excessive smoothing of the traces.

Angular velocity was calculated as the derivative of the joint angles with respect to time. Velocity of the centre of mass in the forward, upward, and medio-lateral directions was calculated using a multi-body kinematic evaluation that calculates the body centre of mass based on the location of the centre of mass of individual segments. The inertial and dynamic parameters of each body segment in the model are scaled based on relative distances between pairs of markers obtained from a motion capture system and the corresponding virtual marker locations in the model implemented in Opensim (Delp et al., 2007), whereas individual body segment masses are scaled with respect to the total body mass. We corrected the medio-lateral velocity data for body side, depending on which foot was positioned in the front start block.

Finally, an inverse dynamic procedure was conducted to calculate the net reaction forces and internal net moments at each of the joints (Delp

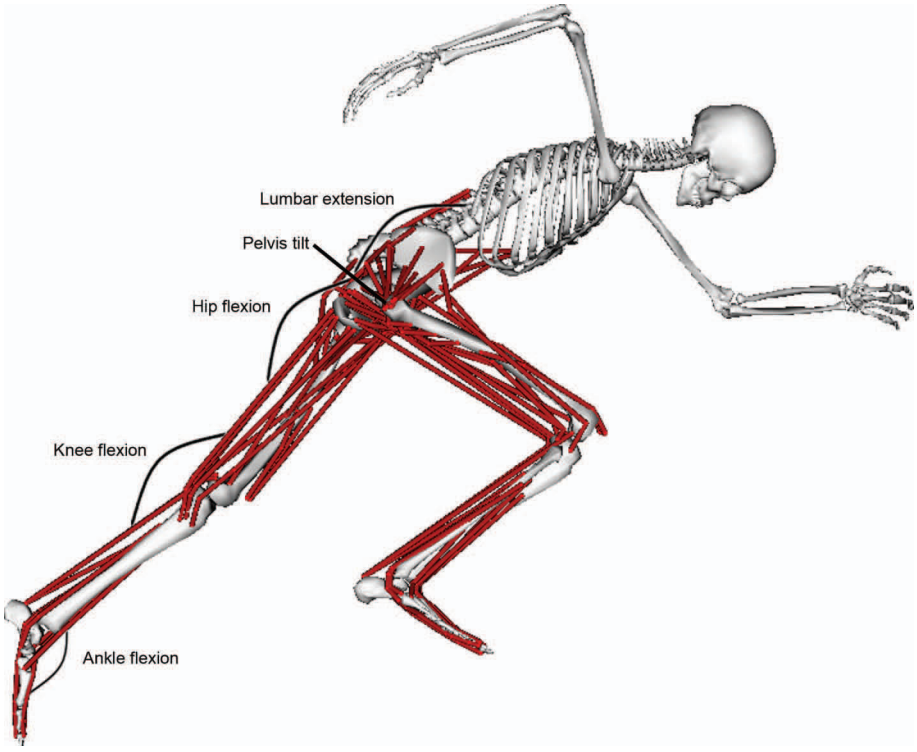

Figure 3. Sagittal joint angle representations. Pelvis tilt represents the absolute orientation in the space; lumbar extension is presented as the angle between the pelvis and the trunk; hip angle as the angle between the pelvis and the thigh; knee angle as the angle between the thigh and the shank; and ankle angle as the angle between the shank and the foot.

et al., 2007). Joint power was calculated by multiplying the joint moment by the relevant joint angular velocity: positive values indicate power generation whereas negative values indicate power absorption. Moment and power data were normalized with respect to body weight (Hof, 1996). No joint moments or powers from the block action were included in the study.

Data analysis

The best of three sprints, based on velocity of centre of mass after second stance, was used for further analysis. Data were time normalized to 100% from the first action after gunshot until the end of the second stance after block clearance, using multipoint cubic splines interpolation. Timing of relevant events was determined based on visual inspection of the marker data on the heel and forefoot (Figure 4). Block clearance was defined as the moment the foot takes off from the block. The contact phase was defined as the moment of touchdown of the foot to the moment the same foot left the ground, i.e. take-off. The flight phase was defined as the period in which no ground contact was made. Touchdown was defined as the first frame in which the athlete's foot made contact with the track, whereas take-off was defined as the first frame in which the foot had fully left the ground or starting block. Mean group averages $\pm$ standard deviations are reported.

Results

Average group velocity is illustrated for the three planes in Figure 5. Forward velocity increased most throughout block clearance (to 3.10 ± 0.25 m $\cdot$ s^{-1}). During the two consecutive support phases, further increases to 4.28 ± 0.27 m $\cdot$ s^{-1} and 5.19 ± 0.30 m $\cdot$ s^{-1} were observed (Figure 5A). Upward velocity increased to 0.73 ± 0.15 m $\cdot$ s^{-1} from the set position to rear block clearance and reached 0.84 ± 0.13 m $\cdot$ s^{-1} when the front foot left the blocks. During the two consecutive stances, vertical velocity increased to 0.67 ± 0.12 m $\cdot$ s^{-1} and 0.70 ± 0.17 m $\cdot$ s^{-1} respectively (Figure 5B). Only minimal medio-lateral velocity was developed (between -0.2 ± 0.13 m $\cdot$ s^{-1} and 0.15 ± 0.1 m $\cdot$ s^{-1}) (Figure 5C).

Sagittal plane graphs of the group mean joint angles, moments, and powers for the rear and front hip, knee, and ankle are shown in Figures 6 and 7 respectively. Figure 8 shows rear and front angular velocity of the hip, knee, and ankle joints. The ankles were dorsiflexed in the set position (rear: $82.5^\circ \pm 7.8^\circ$; front: $82.3^\circ \pm 9.5^\circ$). During block clearance, a small increase in dorsiflexion preceded plantar flexion bilaterally. Maximal plantar flexion was reached at the beginning of the flight phase (front: $133.1^\circ \pm 6.7^\circ$; rear: $139.2^\circ \pm 7.0^\circ$), but reverted towards a dorsiflexed position during flight (first flight: $64.3^\circ \pm 5.9$; second flight: $65.7^\circ \pm 6.3^\circ$). Although the ankle plantarflexed slightly at the end of flight, the ankle was in a dorsiflexed position at initial contact (first stance: $70.6^\circ \pm 5.8^\circ$; second stance: $72.4^\circ \pm 7.1^\circ$). During stance, dorsiflexion increased before reverting into plantarflexion (Figures 6G and 7G). This was initially controlled by power absorption, but was followed by power generation of the plantar flexors (first stance: -0.20 ± 0.03 Nm/N; second stance: -0.23 ± 0.05 Nm/N). Maximal plantarflexion occurred immediately following take-off (first stance: $111.3^\circ \pm 11.2^\circ$; second stance: $107.1^\circ \pm 15.0^\circ$) (Figures 6H, I and 7H, I).

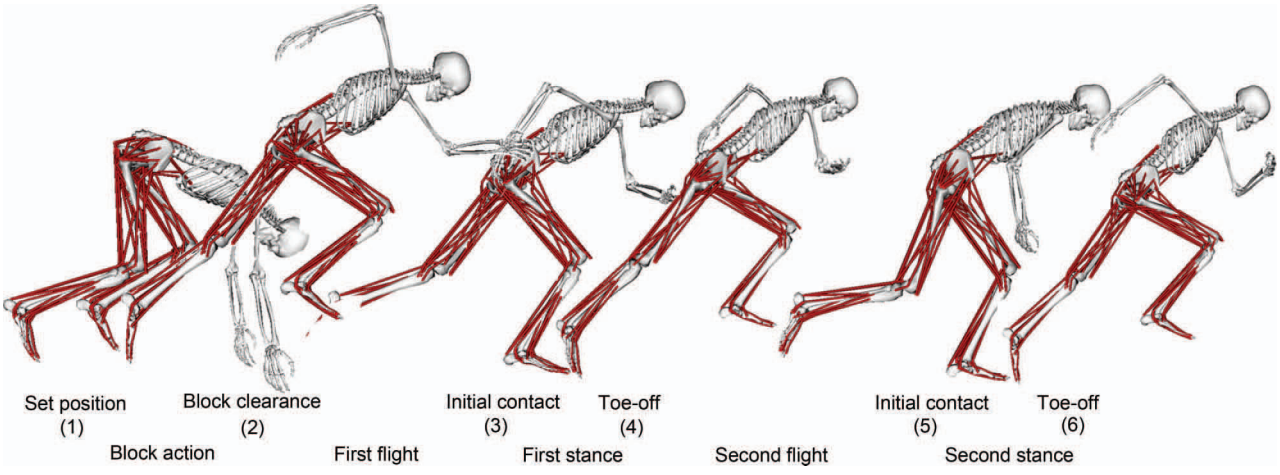

Figure 4. Temporal subdivision. Block clearance is presented as the moment from first action after gunshot, i.e. set position (1) until the foot has left the rear or front block (2). The contact phase is defined as the moment of touchdown of the foot, i.e. initial contact first (3) and second stance (5), to the moment the same foot leaves the ground, i.e. take-off first (4) and second stance (6). The flight phase is defined as the moment of take-off of one foot to the moment of touchdown of the ipsilateral foot.

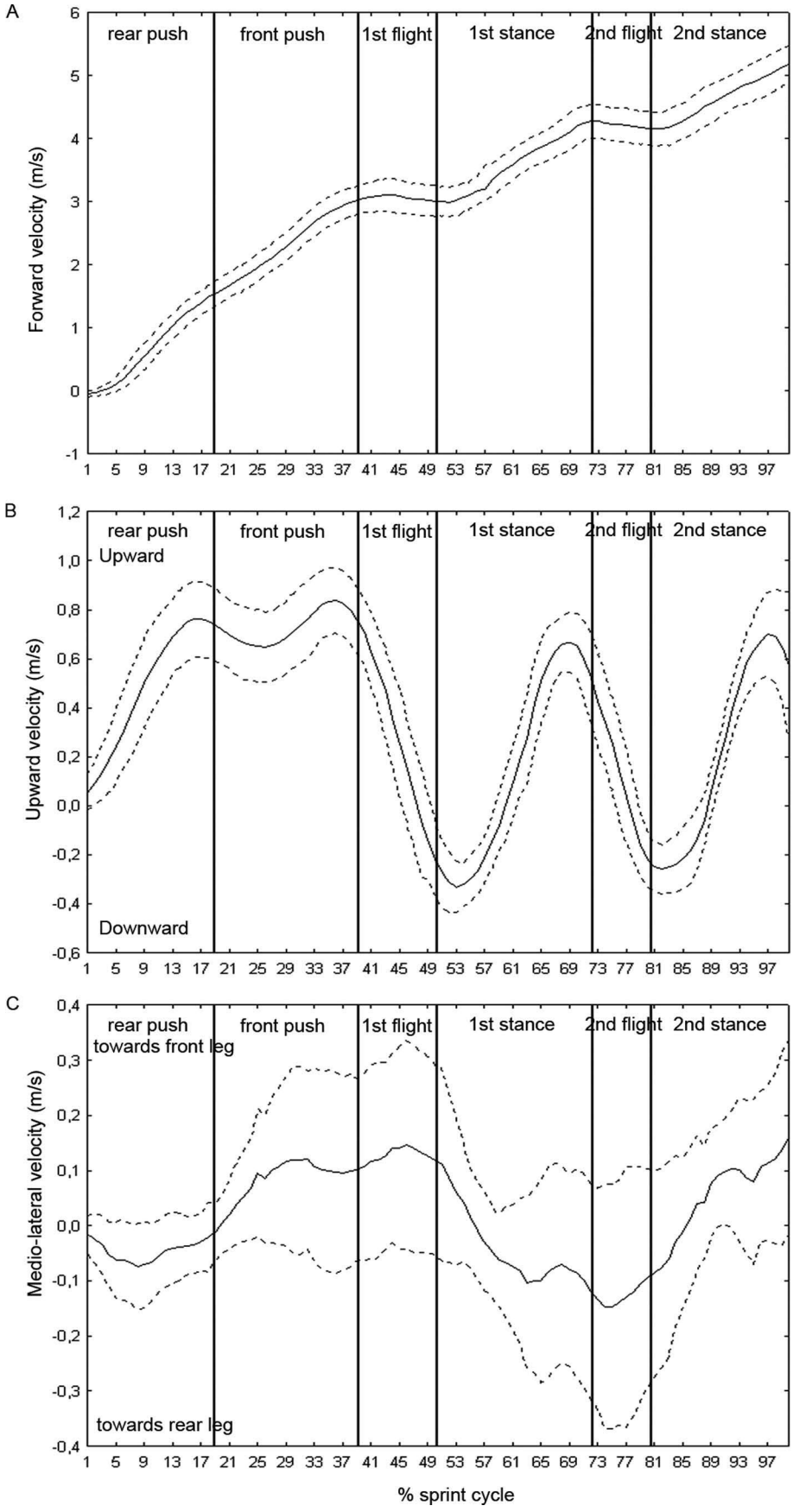

Figure 5. Velocity of the centre of mass in the forward (A), upward (B), and medio-lateral direction (C). Group averages (solid lines) ± standard deviations (dashed lines) are presented. The vertical lines indicate the different phases of the start action.

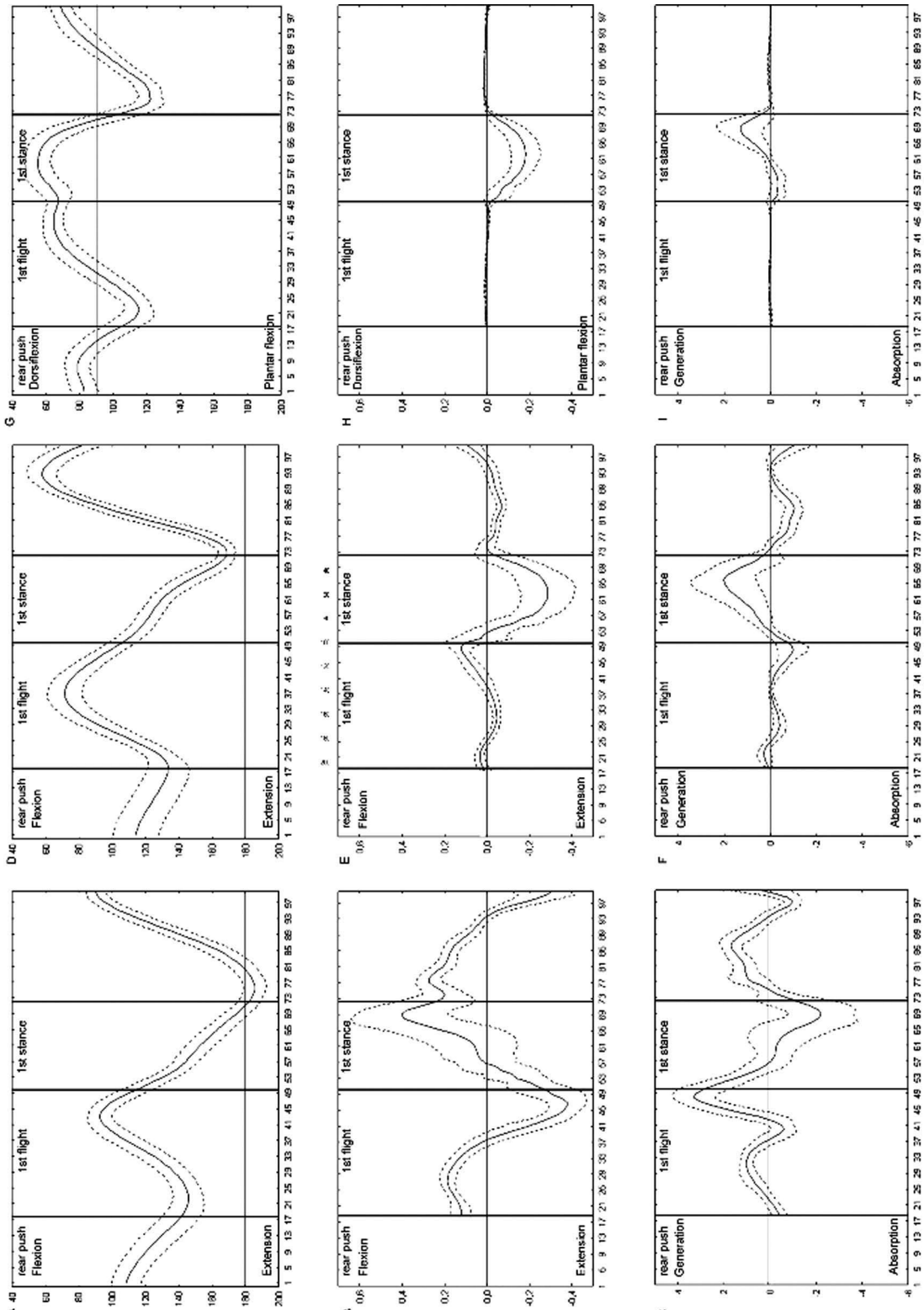

Figure 6. Joint angles, joint moments, and joint power of the sagittal plane of the hip, knee, and ankle of the rear leg. Group averages (solid lines) ± standard deviations (dashed lines) are presented. The vertical lines indicate the block phase, flight phase, and stance phase. Positive angles represent hip flexion, knee flexion, and ankle dorsiflexion. Positive joint moments represent an internal hip extension moment, knee extension moment, and ankle dorsiflexion moment. Positive power represents power generation.

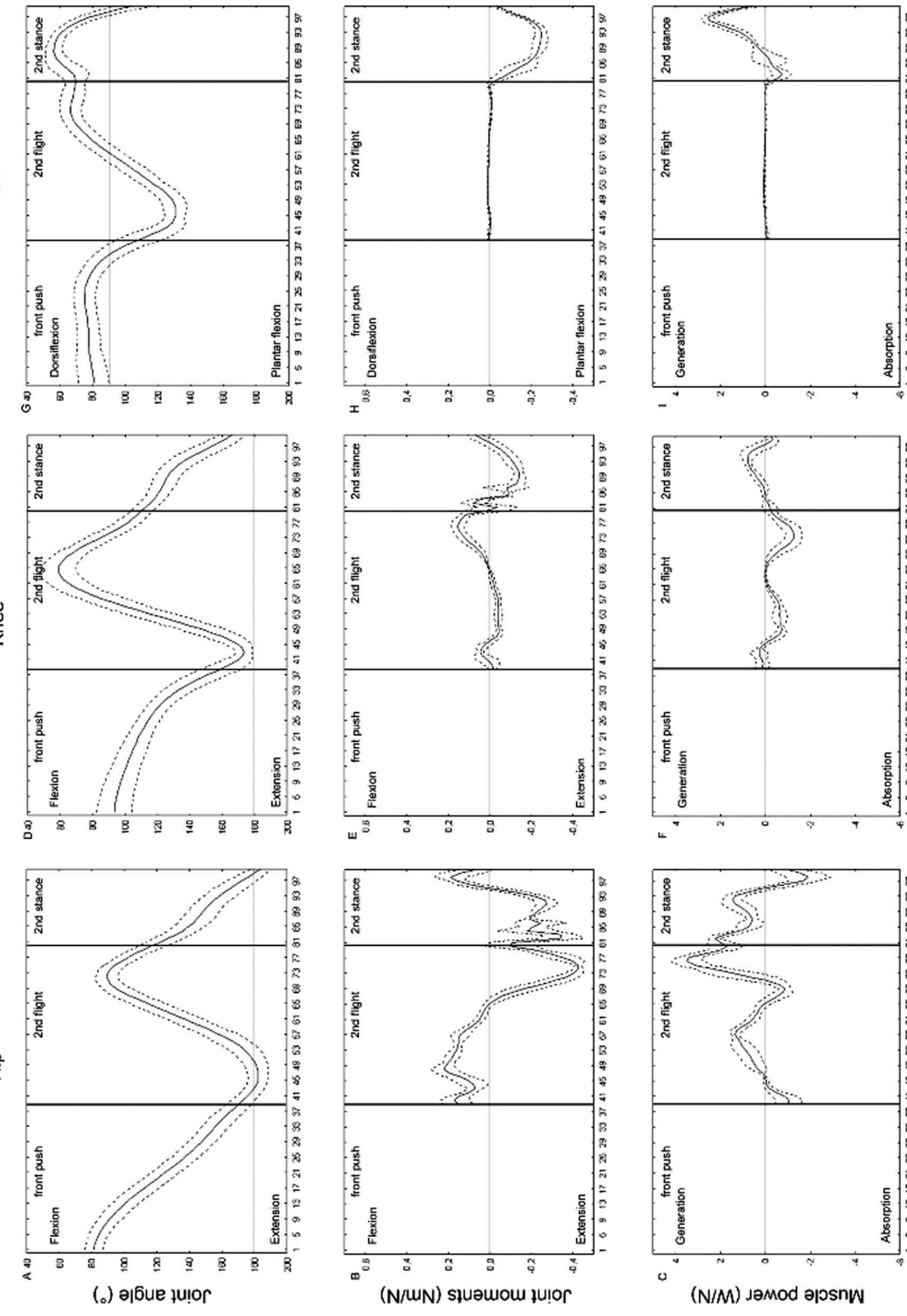

Figure 7. Joint angles, moments, and joint power of the sagittal plane of the hip, knee, and ankle of the front leg. Group averages (solid lines) ± standard deviations (dashed lines) are presented. The vertical lines indicate the block phase, flight phase, and stance phase. Positive joint moments represent an internal hip extension moment, knee extension moment, and ankle dorsiflexion moment. Positive power represents power generation.

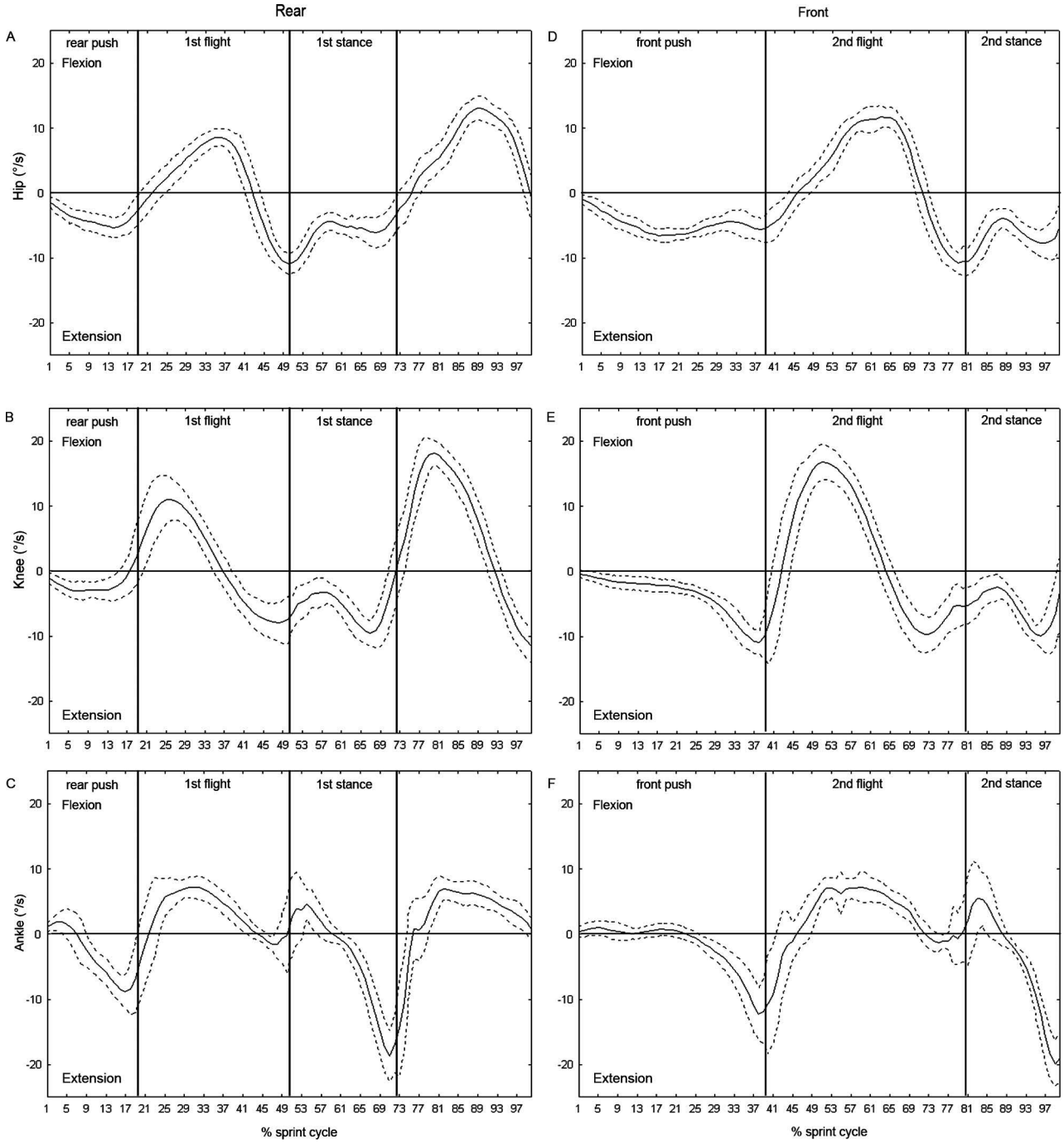

Figure 8. Hip, knee, and ankle joint angular velocity of the rear (left) and front (right) leg. Group averages (solid lines) ± standard deviations (dashed lines) are presented. The vertical lines indicate the block phase, flight phase, and stance phase. Positive values represent angular velocity towards hip flexion, knee flexion, and ankle dorsiflexion.

The knees were flexed in the set position (rear: 112.8° ± 15.1°; front: 94.5° ± 11.2°). Extension occurred during block clearance and reached its maximum at the beginning of the flight phase, with larger extension in the front compared with the rear leg (rear: 134.9° ± 11.2°; front: 177.4° ± 5.2°). During the flight phase, the knees were initially flexed (first flight: 70.1° ± 10.2°; second flight: 58.1° ± 11.4°) (Figures 6D and 7D). This was first induced by power generation of the knee flexor muscles but later controlled by power absorption of the knee extensor muscles (Figures 6E, F and 7E, F). Prior to initial contact, power absorption of the knee flexors prevented excessive extension (first stance: 0.14 ± 0.05 Nm/N; second stance: 0.18 ± 0.02 Nm/N). From a flexed position at initial contact (first stance: 111.6° ± 9.1°; second stance: −115.6° ± 6.2°), the knee extensors generated power to induce extension throughout stance and to attain maximal extension at take-off (first stance:

165.2° ± 20.6°; second stance: 163.6° ± 17.7°; first stance: −0.20 ± 0.04 Nm/N; second stance: −0.10 ± 0.04 Nm/N) (Figures 6D and 7D).

The hip joints were flexed in the set position (rear: 107.1° ± 9.4°; front: 82.8° ± 10.1°) and extended during block clearance to reach maximal extension during the beginning of the flight phase (rear: 146.8° ± 9.4°; front: 183.2° ± 6.8°) (Figures 6A and 7A). Subsequently, power generation of the hip flexors induced flexion (first flight: 90.7° ± 6.6°; second flight: 87.8° ± 6.4°). During the second half of flight, hip flexion was first controlled by power absorption of the hip extensors, after which these muscles generated power to induce hip extension (first stance: −0.33 ± 0.15 Nm/N; second stance: −0.43 ± 0.01 Nm/N) (Figures 6B, C and 7B, C). At initial contact, the hips were in a flexed position (first stance: 121.2° ± 11.3°; second stance: 124.4° ± 11.3°) and continued to extend throughout stance, controlled by power absorption of the hip flexors (first stance: 0.42 ± 0.16 Nm/N; second stance: 0.20 ± 0.06 Nm/N) (Figures 6B, C and 7B, C). Maximal extension was achieved immediately following take-off (of the first stance leg) (first stance: 180.6° ± 20.9°; second stance: 181.1° ± 20.0°) (Figures 6A and 7A).

Focusing on the timing across joints during the first stance, maximal extension of the knee joint was established at take-off (73.1 ± 2.0% of normalized cycle) whereas full extension in the hip (74.9 ± 2.0%) and ankle (75.9 ± 2.1%) was reached shortly after take-off (Figures 6A, D, G). All athletes showed initial peak angular velocity at the hip (51.2 ± 2.1%) just before initial contact of the stance. The knee (67.2 ± 2.1%) and ankle (71.3 ± 1.4%) reached their peak angular velocity prior to toe-off (Figures 8A, B, D). Consequently, peak power generation was observed in the hip prior to initial contact (47.9 ± 1.7%) followed by the knee (66.6 ± 2.2%) and the ankle (69.0 ± 3.1%) prior to take-off (Figures 6C, F, I).

Average joint angles of pelvis tilt and lumbar extension, pelvis rotation and pelvis list, together with front and rear leg hip adduction and rotation are presented in Figure 9. Pelvis tilt changed during transition from block into sprint running into a more upright orientation at block clearance: −37.3° ± 7.0° (after first step: −32.9° ± 5.7°; after second step: −28.9° ± 5.4°). A small reversion at the end of both stances and beginning of flight was seen (Figure 9A). In contrast, lumbar extension was maximal after block clearance (−32.2° ± 8.2°) and during flight (both −29.6° ± 7.8°), but reverted towards flexion at the end of flight and at the beginning of stance (Figure 9D). A wide range of motion in both hip and pelvis rotation and abduction was observed during both the stance and flight phase: hip rotation varied by 17° for the rear leg and 20° for the front; pelvis rotation varied by 33°; hip abduction varied by 21° for the rear leg and 22° for the front leg; and pelvis list varied by 26° (Figures 9B, C, E, F, G, H).

Discussion

This study has highlighted the specific technical skills of well-trained sprinters during the transition from start block to sprint running by providing insights into full three-dimensional kinematic and kinetic characteristics underlying initial sprinting performance during the first steps after block clearance. This phase imposes unique demands on the technical skills of the athlete as the sprinter strives to maximize forward velocity immediately from the set position by a powerful take-off against both starting blocks. After block clearance, the athlete has then to prepare an effective landing to further develop forward acceleration. Our results confirm that the transition from block clearance to sprint running relies on specific technical skills that differ from those previously reported to characterize the second step and the phase of maximal running speed.

During the first step, maximal power is predominately generated by the hip (54%), followed by the knee (31%) and the ankle (15%). This agrees with Charalambous et al. (2012), who also suggested the important role played by the knee during the first stance. The importance of power generation at the knee is specific for this transition from block clearance to sprint running, since from the second stance the knee only accounts for 9% of total power generation and the importance of the ankle increases up to 38% (Figures 6C, F, I and 7C, F, I). This finding agrees with literature presenting similar distribution of power generation during second stance (hip: 35%, knee: 17%, ankle: 48%; Jacobs, 1992), acceleration (hip: 35%, knee: 17%, ankle: 48%; Johnson, 2001), and maximal velocity (hip: 39%, knee: 17%, ankle: 44%; Bezodis et al., 2008). The large contribution of power generation at the knee during the first stance versus the relatively small contribution of the knee during the second stance suggests the need for different technical abilities of the athlete to control the knee action. During the first step, where the sprinter leans forward, active extension of the knee has a greater potential to contribute to forward velocity. During the second step, where the sprinter is in a more erect position, the knee action contributes mainly to upward velocity. Consequently, knee extension is postponed until the body centre of mass progresses sufficiently over the base of support to induce forward acceleration (Jacobs, 1992; Jacobs et al., 1996). This finding illustrates that effective transition from block

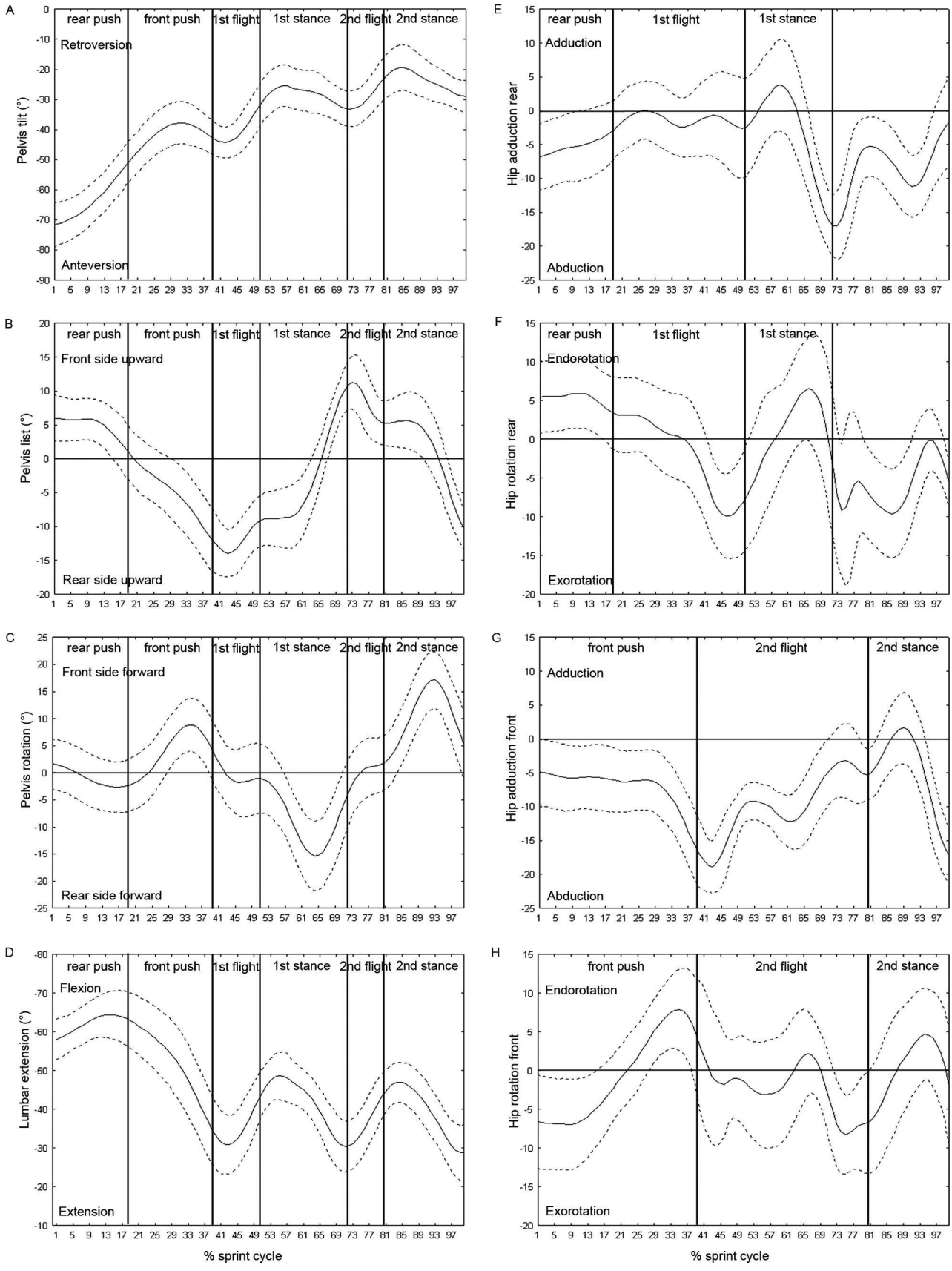

Figure 9. Joint angles of pelvis tilt, list and rotation, lumbar extension (left side), hip adduction and rotation of the rear and front (right side). Group averages (solid lines) ± standard deviations (dashed lines) are presented. The vertical lines indicate the different phases of the start action. Positive angles represent pelvic retroversion, pelvic forward and upward rotation of the side of the front leg, lumbar extension, hip adduction and hip endorotation of the front as well as the rear leg.

clearance to the first stance relies on forceful action of the knee extensors, which becomes less dominant from the second stance onwards since the plantar flexors are in a better position to contribute to forward progression.

During sprint running, athletes use a stretch-shortening mechanism, with eccentric muscle actions preceding concentric actions, to take advantage of the elastic component of muscle action and to enhance muscle force production around the hip, knee, and ankle (Bezodis et al., 2008; Kuitunen, Komi, & Kyröläinen, 2002; Mann & Sprague, 1980; Slawinski et al., 2010b). The existence of the stretch-shortening mechanism during the first steps may be questioned given the specific positional changes of the athlete. Although joint power generation and absorption only indirectly relate to individual muscle action, our findings indicate that during the first steps of sprint running a stretch-shortening mechanism is preserved at the hip and ankle, but not at the knee: at the hip, maximal power generation of the hip extensors is found immediately before and at initial contact where the hip extensors actively pull the body over the touchdown point. During the remainder of stance, power absorption of the hip flexors decelerates hip extension and prepares for forceful power generation of the hip flexors during the first part of the subsequent flight phase (Figure 6C). A similar mechanism is found for the ankle plantar flexors during stance with power absorption preceding the forceful power generation at take-off (Figure 6I). In contrast, no stretch-shortening cycle can be confirmed at the knee. Prior to initial contact, the knee flexors decelerate knee extension. From initial contact onwards, the knee extensors generate power throughout the entire stance phase (Figure 6F). This is in contrast with sprinting at maximal velocity where weight is first counteracted by initial knee flexion and related power absorption (Bezodis et al., 2008; Kuitunen et al., 2002; Mann & Sprague, 1980). No initial knee flexion is found during the first two steps following block clearance. To successfully rise from the flexed position during the first step, the athlete thus invests in immediate power generation of the knee extensors rather than preserving a stretch-shortening cycle. The stretch-shortening mechanism around the hip and ankle, previously reported for other phases of sprint running (Bezodis et al., 2008; Johnson, 2001; Slawinski et al., 2010b) is confirmed during the first two steps. To relate the observed power generation and absorption to eccentric and concentric action of individual muscles and to definitely conclude on the presence of stretch-shortening enhancement, the current findings need to be further supported by other biomechanical parameters such as muscle-tendon length in combination with surface electromyography.

Not only are the distribution and magnitude of power generation important, but also the temporal consequences of strategies at the different joints. The present study shows that both peak angular velocity and peak power generation in the hip are observed before initial contact. Peak angular velocity and peak power generation in both knee and ankle are seen prior to take-off (Figures 8B, C and 6F, I). We therefore suggest a proximal-to-distal timing in the onset of the sprint action, which is in accordance with literature (Bezodis et al., 2008; Charalambous et al., 2012; Jacobs, 1992; Johnson, 2001). During the first part of stance, the hip will pull the body over the touchdown point and therefore minimize braking. Once the centre of mass is ahead of the touchdown point, the knee and ankle will generate power and as a consequence also horizontal velocity. For the kinematics, one can assume that it is advantageous to have maximal limb extension at take-off as this maximizes step length. Therefore, we expected maximal extension of all three joints at take-off. This was however only confirmed for the knee joint. Both hip and ankle reached maximal extension after take-off. Despite the short duration of the flight phase, athletes choose to invest in additional power absorption of the hip flexors as part of the stretch-shortening cycle and postpone active hip flexion (Figure 6C).

During the sprint start, the athlete rises from the set position in the blocks to a forward leaning position and develops both horizontal and vertical velocity. The mechanisms contributing to the rise are clearly different between the block phase and the first two steps. During block clearance, extension of the lower limb joints together with lumbar extension induces a more upright orientation of the sprinter. In contrast with block clearance, only extension of the lower limb joints contributes to a more upright position during the two subsequent steps. During these steps, limb extension is accompanied by lumbar flexion, which only reverses towards extension during flight (Figures 6A, D, G and 9D). We therefore conclude that trunk extension only assists the rise of the athlete during the block phase. The opposite action of the trunk and lower limbs during the first steps seems to suggest that the sprinter actively searches for a more bent trunk position during transition to maximize the generation of horizontal velocity. This suggests a greater forward lean is associated with a larger and more forward orientated ground reaction force as well as with a larger forward velocity (Hunter, Marshall, & McNair, 2005; Kugler & Janshen, 2010; Morin, Edouard, & Samozino, 2011).

Previously, the sprint start was mainly considered a two-dimensional action (Charalambous et al., 2012; Coh et al., 2007; Jacobs, 1992; Mero, Luhtanen, & Komi, 1983; Slawinski et al., 2010a,

2010b). In contrast, our results show a considerable range of motion in hip and pelvis rotation as well as abduction (Figures 9B, C, E, F, G, H). The considerable hip abduction range of motion combined with the limited medio-lateral velocity is indicative of an effective compensatory mechanism present in well-trained athletes to minimize the effect of the lateral foot positioning on the medio-lateral velocity of the centre of mass. By minimizing the medio-lateral velocity of the pelvis, the development of forward velocity of the centre of mass seems to be optimized (Figures 5A, C).

Conclusion

The transition from start block to sprint running requires specific technical skills to achieve maximal forward acceleration. This study primarily highlights the significant and phase-specific role of the knee muscles in obtaining an effective transition from block clearance to sprint running: Whereas during the first part of the first stance, the hip pulls the body over the touchdown point, the knee extensors will contribute to generation of joint power and consequently horizontal velocity. In contrast to the hip and ankle joint, no stretch-shortening enhancement can be confirmed at the knee during this transition phase. Furthermore, during the transition phase, the sprinter actively prepares for a more forward leaning position to maximize horizontal velocity generation.

References

Bezodis, I., Kerwin, D.G., & Salo, A. (2008). Lower-limb mechanics during the support phase of maximum-velocity sprint running. *Medicine and Science in Sports and Exercise*, *40*, 707–715.

Bezodis, N.E., Salo, A.I.T., & Trewartha, G. (2010). Choice of sprint start performance measure affects the performance-based ranking within a group of sprinters: Which is the most appropriate measure? *Sports Biomechanics*, *9*, 258–269.

Charalambous, L., Irwin, G., Bezodis, I., & Kerwin, D.G. (2012). Lower limb joint kinetic and ankle joint stiffness in the sprint start push-off. *Journal of Sports Sciences*, *30*, 1–9.

Coh, M. (2006). The biomechanical model of the sprint start and block acceleration. *Facta Universitatis: Series Physical Education & Sport*, *4*, 103.

Coh, M., Bojan, J., Branko, S., Tomazin, K., & Dolenec, A. (1998). Kinematic and kinetic parameters of the sprint start and start acceleration model of top sprinters. *Gymnica*, *28*, 33–41.

Coh, M., Milanovic, D., & Kampmiller, T. (2001). Morphological and kinematic characteristics of elite sprinters. *Collegium Antropologicum*, *25*, 605–610.

Coh, M., Peharec, S., & Bacic, P. (2007). The sprint start: Biomechanical analysis of kinematic, dynamic and electromyographic parametres. *New Studies in Athletics*, *22*, 29–38.

Coh, M., & Tomazin, K. (2006). Kinematic analysis of the sprint start and acceleration from the blocks. *New Studies in Athletics*, *21*, 23–33.

Delp, S.L., Anderson, F.C., Arnold, A.S., Loan, P., Habib, A., John, C.T. et al. (2007). OpenSim: Open-Source software to create and analyze dynamic simulations of movement. *IEEE Transactions on Biomedical Engineering*, *54*, 1940–1950.

Golden, G.M., Pavol, M.J., & Hoffman, M.A. (2009). Knee joint kinematics and kinetics during a lateral false-step maneuver. *Journal of Athletic Training*, *44*, 503–510.

Hamner, S.R., Seth, A., & Delp, S.L. (2010). Muscle contributions to propulsion and support during running. *Journal of Biomechanics*, *43*, 2709–2716.

Hof, A.L. (1996). Scaling gait data to body size. *Gait and Posture*, *4*, 222–223.

Hoyt, D.F., Wickler, S.J., & Cogger, E.A. (2000). Time of contact and step length: The effect of limb length, running speed, load carrying and incline. *Journal of Experimental Biology*, *203*, 221–227.

Hunter, J.P., Marshall, R.N., & McNair, P.J. (2005). Relationships between ground reaction force impulse and kinematics of sprint-running acceleration. *Journal of Applied Biomechanics*, *21*, 31–43.

Jacobs, R. (1992). Intermuscular coordination in a sprint push-off. *Journal of Biomechanics*, *25*, 953–965.

Jacobs, R., Bobbert, M., & Van Inghen Schenau, G.J. (1996). Mechanical output from individual muscles during explosive leg extensions: The role of biarticular muscles. *Journal of Biomechanics*, *29*, 513–523.

Johnson, M.D. (2001). Muscle power patterns in the mid-acceleration phase of sprinting. *Journal of Sports Sciences*, *19*, 263–272.

Kugler, F., & Janshen, L. (2010). Body position determines propulsive forces in accelerated running. *Journal of Biomechanics*, *43*, 343–348.

Kuitunen, S., Komi, P.V., & Kyröläinen, H. (2002). Knee and ankle joint stiffness in sprint running. *Medicine and Science in Sports and Exercise*, *34*, 166–173.

Mann, R., & Sprague, P. (1980). A kinetic analysis of the ground leg during sprint running. *Research Quarterly in Exercise and Sport*, *51*, 334–348.

Mann, R.V. (1981). A kinetic analysis of sprinting. *Medicine and Science in Sports and Exercise*, *13*, 325–328.

Marfell-Jones, M., Olds, T., Steward, A., & Carter, L. (2006). *International standards for anthropometric assessment*. Potchefstrom: ISAK.

Mero, A. (2006). Effects of muscle–tendon length on joint moment and power during sprint starts. *Journal of Sports Sciences*, *24*, 165–173.

Mero, A., Luhtanen, P., & Komi, P.V. (1983). A biomechanical study of the sprint start. *Scandinavian Journal of Sport Sciences*, *5*, 20–28.

Morin, J., Edouard, P., & Samozino, P. (2011). Technical ability of force application as a determinant factor of sprint performance. *Medicine and Science in Sports and Exercise*, *43*, 1680–1688.

Salo, A., Bezodis, I., Batterham, A.M., & Kerwin, D.G. (2011). Elite sprinting: Are athletes individually step frequency or step length reliant? *Medicine and Science in Sports and Exercise*, *43*, 1055–1062.

Slawinski, J., Bonnefoy, A., Leveque, J.M., Ontanon, G., Riquet, A., Dumas, R. et al. (2010a). Kinematic and kinetic comparisons of elite and well-trained sprinters during sprint start. *Journal of Strength and Conditioning Research*, *24*, 896–905.

Slawinski, J., Bonnefoy, A., Ontanon, G., Leveque, J.M., Miller, C., Riquet, A. et al. (2010b). Segment-interaction in sprint start: Analysis of 3D angular velocity and kinetic energy in elite sprinters. *Journal of Biomechanics*, *43*, 1494–1502.